JUPITER S-BURST POLARIZATION MEASUREMENTS USING THE WAVEFORM RECEIVER

U. Taubenschuss*, H. O. Rucker*, and W. Macher*

Abstract

Jupiter S-bursts emerging from an Io-B radio storm were recorded using a waveform receiver. On the basis of the signal's waveform all four Stokes parameter spectra were determined with a time resolution of 0.8 ms and a frequency resolution of 12.5 kHz. Io-B S-bursts were found to be 100% elliptically right-handed polarized. The degree of polarization depends on S-burst intensity which is due to the depolarizing influence of the background. In consideration of this result the corresponding values for the degree of total polarization (d) and the degrees of linear (d_l) and circular (d_c) polarization are: $d = 0.97$, $d_l = 0.82$ and $d_c = 0.53$. Further on, the influence of the Faraday effect was investigated. It was found that the polarization ellipse undergoes more than 100 half-rotations at 15 MHz and the orientation of the ellipse's semimajor axis at the source region is nearly parallel to the orientation of the local magnetic field. Moreover, a change of the ellipse's ellipticity with frequency indicates a changing geometry between the source region and a distant observer.

1 Data preparation and Stokes parameters

The Lustbühel radio station located on the outskirts of Graz, Austria, is equipped with two logarithmic periodic antennas, one at the east side and one at the west side of the main observatory building. They are sensitive in the frequency range from 13 – 32 MHz and due to the fact that the antenna polarization planes are oriented perpendicular to each other, polarization measurements can be performed. As receivers, the Digital Spectropolarimeter (DSP) [Rucker *et al.*, 2001] in combination with the Waveform Receiver (WFR) [Leitner, 2001] are used. The WFR samples the baseband signal from the DSP with a sampling rate of 25 MHz (two channels simultaneously) and stores the sampled waveform to a harddisk. About 6.3 seconds of observation result in a file size of 604 MB.

* *Space Research Institute, Austrian Academy of Sciences, Schmiedlstrasse 6, A-8042 Graz, Austria*

The two WFR-sampled and digitally stored voltage signals from the East- and the West-antenna serve as input signals for polarization analysis. Since computation of the Stokes parameters requires complex signals, the so-called *analytic signals* have to be generated first [Born and Wolf, 1965]. For two linearly polarized antennas, the four Stokes parameters S, Q, U and V, which completely describe the state of polarization, are defined as

$$S = \langle |E_x(t)|^2\rangle + \langle |E_y(t)|^2\rangle = \langle E_x(t) \cdot E_x^*(t)\rangle + \langle E_y(t) \cdot E_y^*(t)\rangle \quad (1)$$
$$Q = \langle |E_x(t)|^2\rangle - \langle |E_y(t)|^2\rangle = \langle E_x(t) \cdot E_x^*(t)\rangle - \langle E_y(t) \cdot E_y^*(t)\rangle \quad (2)$$
$$U = 2 \cdot \langle |E_x(t)| \cdot |E_y(t)| \cdot \cos(\Delta\varphi)\rangle = 2 \cdot \Re\{\langle E_x(t) \cdot E_y^*(t)\rangle\} \quad (3)$$
$$V = 2 \cdot \langle |E_x(t)| \cdot |E_y(t)| \cdot \sin(\Delta\varphi)\rangle = 2 \cdot \Im\{\langle E_x(t) \cdot E_y^*(t)\rangle\} \quad (4)$$

The brackets $\langle \ldots \rangle$ indicate the time average operator, $E_x(t)$ and $E_y(t)$ are the analytic signals of the sampled waveforms from the East- and the West-antenna, respectively, and $\Delta\varphi = \varphi_x - \varphi_y$ indicates their phase difference.

A geometric correction has to be applied on the waveform signals from the Lustbühel antenna system because the antennas are fixed in azimuth and elevation and do not track the radio source in the sky. This is done by applying an appropriate rotation matrix on $E_x(t)$ and $E_y(t)$ before starting the periodogram computations.
On the basis of the found Stokes parameters S, Q, U and V other useful quantities can be derived [Kraus, 1986]:

$$\text{degree of polarization} \quad d = \left(\sqrt{Q^2 + U^2 + V^2}\right)/S \qquad (0 \leq d \leq 1) \quad (5)$$
$$\text{degree of linear polarization} \quad d_l = \left(\sqrt{Q^2 + U^2}\right)/S \qquad (0 \leq d_l \leq 1) \quad (6)$$
$$\text{degree of circular polarization} \quad d_c = V/S \qquad (-1 \leq d_c \leq 1) \quad (7)$$
$$\text{tilt angle} \quad \tau = 0.5 \cdot \arctan(U/Q) \qquad (-45^\circ \leq \tau \leq +45^\circ) \quad (8)$$
$$\text{ellipticity} \quad \varepsilon = 0.5 \cdot \arcsin(V/S) \qquad (-45^\circ \leq \varepsilon \leq +45^\circ) \quad (9)$$

According to the IEEE standard [1977] $V > 0$ means right-handed polarization and $V < 0$ means left-handed polarization. Care should be taken that some literature could use an older definition from traditional optics resulting in just the opposite sense of rotation. The tilt angle τ is counted counterclockwise from the horizontal direction, i. e. from the positive x-axis (East antenna) towards the semimajor axis of the polarization ellipse.

2 Analysis

On the basis of equations (1) – (4) the Stokes parameter spectra were calculated, leading to four matrices which contain the values of the Stokes parameters as a function of time and frequency. In the next step, the traces of S-bursts in the S-spectrum were scanned digitally on screen using the PC-mouse. Afterwards, scanned times and frequencies of S-bursts were associated to the four Stokes parameter matrices and for every scanned point a set of S, Q, U and V was obtained. These data were taken for subsequent statistics. This procedure was applied to two WFR data files recorded on February 17, 2004 at 22:39:31 UT and at 23:01:04 UT. The first data file will be referred to as *file1* (the earlier one) and the second one as *file2* (the later one). These files were selected because they store about 12.6 seconds (1.2 GBytes) of excellent S-burst activity arising from an Io-B storm between 14.5 MHz – 24 MHz. At this time, Jupiter was positioned in the middle south-eastern night sky as seen from Lustbühel observatory and the observations were performed around $CML = 151°$, $\Phi_{Io} = 79°$ for *file1* and around $CML = 162°$, $\Phi_{Io} = 81°$ for *file2*. *file1* stores about 80 linear S-bursts and also 7 narrowband burst features. *file2* contains only about 70 linear S-bursts. The mean number of scanned points per S-burst is about 120 and the mean number of scanned points per narrowband burst is about 4280.

Figure 1 displays the occurrence probabilities of d, d_l and d_c. The left column belongs

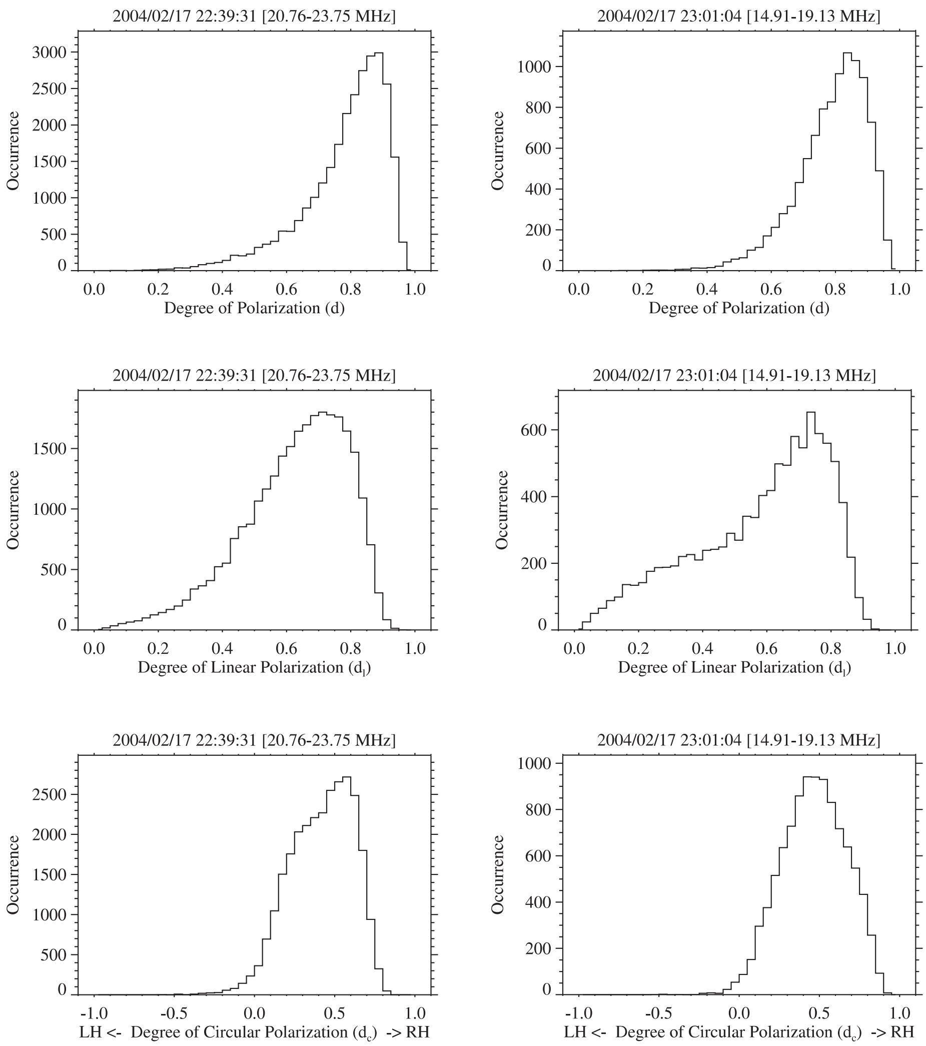

Figure 1: A comparison of the occurrence probabilities of d, d_l and d_c from the two waveform recordings at 22:39:31 UT (left column) and 23:01:04 UT (right column).

to *file1* between 20.7 – 23.8 MHz. The right column belongs to *file2* which was recorded at a lower frequency range between 14.9 – 19.2 MHz. For *file1* the peaks in occurrence probability are $d = 0.88$, $d_l = 0.72$ and $d_c = 0.54$. *file2* yields slightly different values: $d = 0.83$, $d_l = 0.74$ and $d_c = 0.47$. Both data files show a dominantly right-handed elliptical polarization as expected for Jovian Io-B radiation.

2.1 Influence of the background

Next, the degree of polarization was investigated as a function of S-burst intensity, i. e. as a function of Stokes parameter S. The result for *file2* is shown at the left side of Figure 2. The displayed intensity range in dB was subdivided into 50 bins, and for every bin the mean value of d was calculated and plotted as a dark dot into the diagram. Standard deviations for every bin are indicated by vertical bars. As can be seen, the degree of

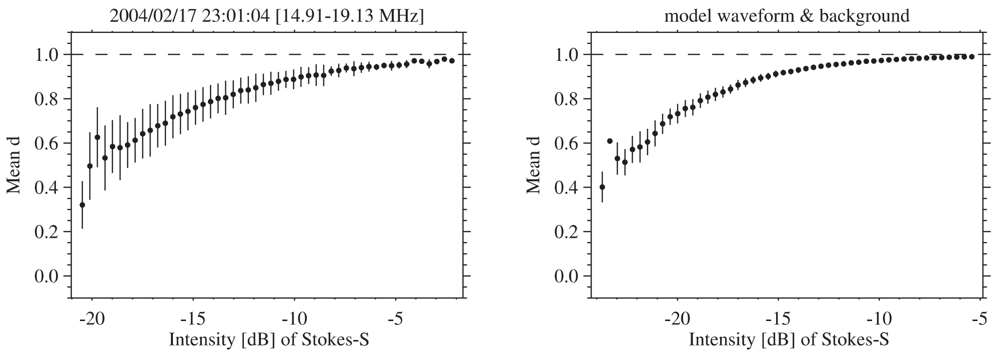

Figure 2: The degree of polarization as a function of intensity for real measured S-burst data (left) and artificially generated model data (right).

polarization increases with increasing S-burst intensity and approaches a value above 95% for highest intensities. This behavior can be explained by the depolarizing influence of the background fluctuations which is more dominant at weaker S-burst intensities. For demonstration the degree of polarization of a model signal is plotted at the right side of Figure 2. This model signal consists of a waveform which is a composition of several single waveforms at successively increasing monochromatic frequencies. Moreover, the waveform amplitudes are linearly increasing with time to simulate the presence of different signal intensities. Finally, a totally unpolarized background signal with randomly distributed phases and intensities was generated and added to the pristine signal waveform. The similarities between real data shown on the left side and model data on the right side are evident which confirms that the nearly perfect polarization of S-bursts gets destroyed by the influence of background fluctuations and partially by mixing and filtering operations in the analogue as well as in the digital domain.

Not only d but also d_l and d_c are increasing with increasing S-burst intensities. Taking the respective maximum values if plotted as a function of Stokes parameter S one gets for both data files: $d = 0.97$, $d_l = 0.82$ and $d_c = 0.53$.

2.2 Influence of the Faraday effect

If an electromagnetic wave enters a birefringent medium it splits into two modes of propagation exhibiting different phase velocities according to their dispersion relations and different polarizations of opposite polarization senses. Thus, they superpose with different phase angles at the antenna system and generate an elliptically polarized wave whose semimajor axis is tilted by the angle $\tau = \frac{\Delta\varphi}{2}$ with respect to a direction defined by the antenna system. If the radio frequency changes, the tilt angle τ changes, too.
Figure 3 displays scanned τ-values as a function of frequency calculated according to equation (8) and transformed into the range $0° - 180°$. For every discretely existing frequency along the frequency axis all τ-values are collected and the median of this group of values is plotted as a dark dot into the diagram. The period $180° - 0°$ is called one *half-rotation*.

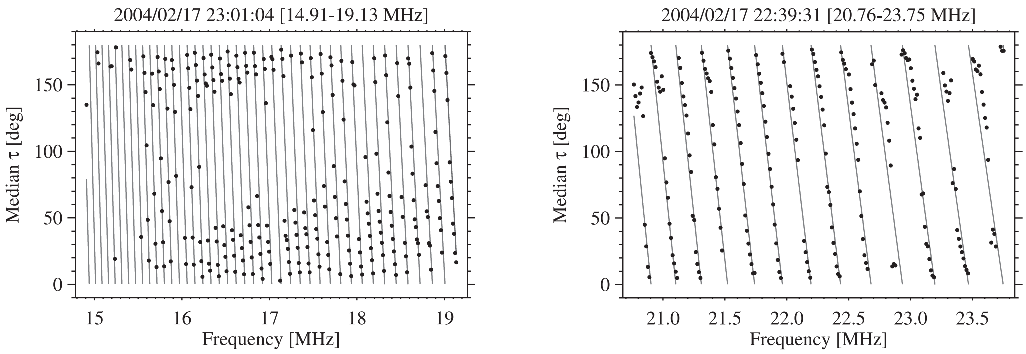

Figure 3: For file2 (left) scanned τ-values trace over 40 half-rotations between $14.9 - 19.1$ MHz. file1 (right) includes about 13 half-rotations ($20.75 - 23.75$ MHz). Solid lines indicate the quadratic fit. According to theory, the spacing between lines increases with increasing frequency.

Solid lines in Figure 3 indicate the fit of the data to the quadratic formula

$$\Omega = C_0 + \frac{C_1}{\nu^2} + \frac{C_2}{\nu^4} \tag{10}$$

This formula was introduced by Boudjada and Lecacheux [1991] and is a simplified description for the full number of half-rotations Ω as a function of the three parameters C_0, C_1 and C_2. C_0 is the original angle τ given at the source region without any Faraday rotation influence. C_1 represents the proper Faraday rotation, i. e. the increase of τ in the media of wave propagation depending on the orientation and magnitude of the magnetic field and the electron content along the ray path [Rohlfs, 1986]. Therefore, quasi-longitudinal propagation is assumed and the plasma frequency must be much lower than the radio frequency. C_2 introduces a correction to the change of τ due to the fact that the X-mode and the O-mode are refracted along different curved ray paths through non-uniformly distributed media [Ross, 1965]. According to Warwick and Dulk [1964] at least 90% of the Faraday effect occur in the terrestrial ionosphere and only 10% can be attributed to plasma inside Jupiter's magnetosphere. Later on, these results were confirmed by Ladreiter *et al.* [1995].

A closer look at Figure 3 reveals that the τ-values seem to undergo a quasi-periodic modulation within one lane if compared to the quadratic fit. This modulation can be modelled by assuming a different power response of the vertical antenna if compared to the horizontal antenna and an additional phase shift between both antennas. The most probable reason for this is that the effective axis of the vertical antenna is not oriented exactly orthogonal to the effective axis of the horizontal antenna. This introduces a difference in power response and a phase shift which vary with observed frequency. So, we are dealing with an antenna system which is not calibrated very well. This fact has to be considered in the interpretation of the results.

3 Interpretation

Figure 4 displays all τ-values of all half-rotations aligned along the curve of the quadratic fit (grey solid line) according to formula (10). τ is given in number of half-rotations and calibrated to absolute zero. At first, the parameters of the fit are determined relative

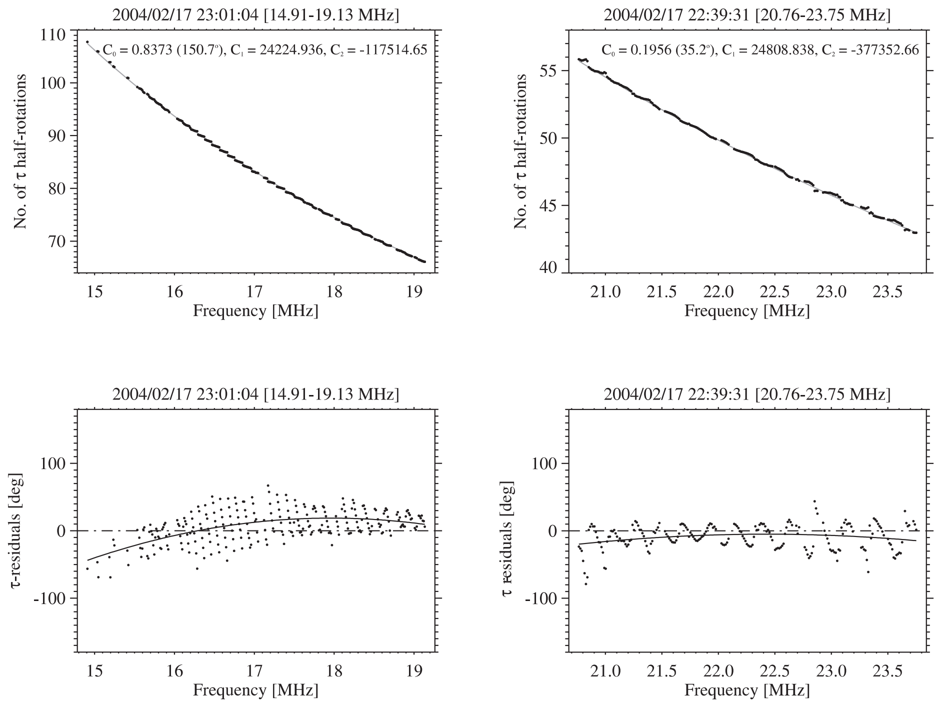

Figure 4: The number of half-rotations performed by the polarization ellipse as a function of frequency for file2 (upper left) and file1 (upper right). The residuals of measured τ to fitted τ are plotted as black dots below. The solid line indicates the smoothed trend.

to an arbitrary level because the absolute zero level is unknown. If $\nu \to \infty$ is inserted into formula (10), it reads $\Omega = C_0$. So, C_0 actually reflects the number of half-rotations between the arbitrarily selected zero level and a level at which the $\Omega(\nu)$-curve approaches a constant value. Consequently, the round up of $|C_0|$ exhibits the integer number of half-rotations which have to be subtracted from the arbitrarily selected zero level to end up at

the absolute zero level. As can be seen from Figure 4, an S-burst frequency at 14.9 MHz (*file2*) undergoes more than 100 half-rotations during its propagation from the source region towards the antenna system.
Besides the determination of the absolute number of half-rotations, the coefficients of the quadratic fit yield additional information. The parameters C_1 and C_2 consider ionospheric conditions and are beyond the scope of this analysis. C_0 enables a determination of the original orientation of the polarization ellipse given at the source region. Therefore, the angle τ, which is measured with respect to the horizontal direction at the observing site, has to be transformed into a jovicentric system. If this is done, $C_0 = 158.8°$ for *file2* results in an angle of $\tau_j = +24.8°$. Here, τ_j is counted eastwards starting from Jupiter's north pole and is referred to the frequency range of $14.9 - 19.1$ MHz. This result is in agreement with previous studies [Boudjada and Lecacheux, 1991] and indicates a quasi-parallel orientation of the semimajor axis of the polarization ellipse to the direction of the magnetic field $\vec{B}$ given at the Io-B source region. For *file1* ($C_0 = 35.2°$, $\nu = 20.7 - 23.7$ MHz) we get a quite contradictory τ_j of 77.2° which means a more perpendicular orientation of the ellipse's semimajor axis to $\vec{B}$. The reason for this discrepancy is due to the fact that the coefficients for the quadratic fit were determined on the basis of τ-values which are heavily alienated by the poorly calibrated antenna system. *file1* contributes only 13 half-rotations which is far too little to be able to calculate an exact value for C_0. However, the lower graphics in Figure 4 show that the residuals of both fits are by no means randomly distributed which should be the case for a sufficient accurate fit. The authors propose to handle results derived for the orientation of the polarization ellipse with care. Nevertheless, results for the total number of half-rotations are reliable since their calculations are more robust against errors introduced by the antenna system.

Another interesting source characteristics can be deduced if the ellipticity ε is analyzed as a function of frequency (see Figure 5). First of all, it is evident that the Faraday

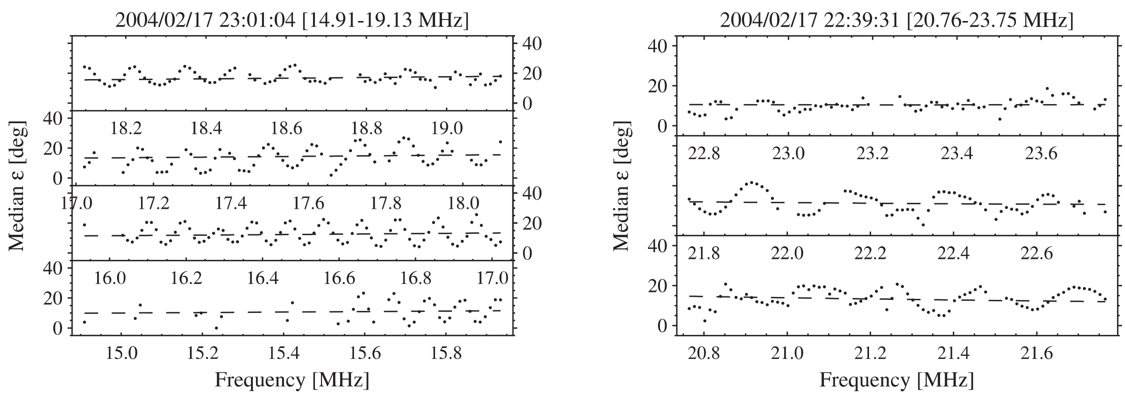

Figure 5: The ellipticity ε of the polarization ellipse as a function of frequency. Every single dot represents the median of a group of ε-values at a certain discrete frequency. The smoothed trend is indicated by a regressive fit (dashed line).

rotation in combination with a poorly calibrated antenna system causes a quasi-periodic modulation of ε with frequency. For *file1* ε is nearly constant around 13° in the frequency range 20.7 – 23.7 MHz. On the contrary, the regressive fit (dashed line) to ε in *file2* is slightly decreasing with decreasing frequency from about 18° at 19.13 MHz towards 10° at 14.91 MHz. This dependence can be explained by geometrical considerations since the cyclotron maser theory predicts that ε of the polarization ellipse is related to the beaming angle θ by [Dulk *et al.*, 1994]

$$\cos(\theta) = \tan(\varepsilon) \tag{11}$$

An ε from 18° – 10° corresponds to a θ from 71.0° – 79.8°. Now, imagine a non-maxwellian electron population propagating upwards along a magnetic flux tube which is bending away from the observer. If the radiation remains to be visible from higher towards lower frequencies, θ must increase as the magnetic flux tube is bending away.

References

Born, M., and E. Wolf, Principles of Optics, Pergamon, Oxford, 1965.

Boudjada, M. Y., and A. Lecacheux, Faraday rotation of Jupiter's decametric radiation, *Astron. Astrophys.*, **247**, 235-246, 1991.

Dulk, G. A., Y. Leblanc, and A. Lecacheux, The complete polarization state of Io-related radio storms from Jupiter: a statistical study, *Astron. Astrophys.*, **286**, 683-700, 1994.

IEEE, Standard Definitions of Terms for Radio Wave Propagation, Std. 211-1977, Institute of Electrical and Electronics Engineers, New York, 1977.

Kraus, J. D., Radio Astronomy *2nd edition*, Cygnus-Quasar Books, 1986.

Ladreiter, H. P., G. Litvinenko, M. Y. Boudjada, and H. O. Rucker, Faraday rotation in Jupiter's decametric radio emission used for remote sensing of the terrestrial ionosphere and the emission's source region at Jupiter, *Planet. Space Sci.*, **43**, 1595-1605, 1995.

Leitner, M., Waveform analysis techniques of Jovian S-burst observations, PhD-Thesis, University of Graz, 2001.

Rohlfs, K., Tools of radio astronomy, Springer Verlag, 1986.

Ross, W. J., Second-order effects in high-frequency transionospheric propagation, *J. Geophys. Res.*, **70**, 597, 1965.

Rucker, H. O., A. Lecacheux, A. A. Konovalenko, and M. Leitner, New frontiers in decameter radio astronomy, in *Planetary Radio Emissions V*, Rucker H. O., Kaiser M. L., Leblanc Y. (eds.), Austrian Academy of Sciences Press, Vienna, 51–61, 2001.

Warwick, J. W., and G. A. Dulk, Faraday rotation on decametric radio emission from Jupiter, *Science*, **145**, 380, 1964.